Collider signatures of a scalar leptoquark and vectorlike lepton in light of muon anomaly

Nivedita Ghosh,[1,*] Santosh Kumar Rai,[1,†] and Tousik Samui[2,‡]

[1]*Regional Centre for Accelerator-Based Particle Physics Harish-Chandra Research Institute, A CI of Homi Bhabha National Institute, Chhatnag Road, Jhunsi, Prayagraj 211019, India*
[2]*Department of Physical Sciences, Indian Institute of Science Education and Research Kolkata, Mohanpur 741246, India*

(Received 13 July 2022; accepted 31 January 2023; published 23 February 2023)

Despite the immense success of the Standard Model (SM), the hunt for physics beyond the Standard Model (BSM) has continued. Extension of the SM gauge group or the particle content of the SM remains a viable solution to many observed anomalies, such as the anomalous magnetic moment of muon, flavor violation, dark matter, etc. In this work, we consider a BSM model which includes a leptoquark, a vectorlike lepton, and a real scalar singlet. The model accounts for a dark matter candidate through a $\mathbb{Z}_2$ symmetry in addition to predicting the muon $(g-2)$ in agreement with the experimental measurement. We also show that the experimental measurements of the lepton flavor violation are satisfied in a wide range of parameter space. The viable parameter space of the model is used to study the collider signatures arising from the pair production of the leptoquark in the $2\mu + 2b + \not{E}_T$ channel at the 14 TeV LHC run.

DOI: 10.1103/PhysRevD.107.035028

I. INTRODUCTION

The success of the Standard Model (SM) predictions of particle physics is astonishingly precise. All the predicted particles have been observed in various experiments. The last particle to be discovered is the Higgs boson [1,2]. Despite its huge success, it has limitations in explaining several anomalies observed in precision measurements and other experiments [3–9]. These limitations include neutrino mass and mixing observations, dark matter (DM) in the universe, several anomalies in the flavor sector, and $(g-2)_\mu$ anomaly, among many others. The quest for physics beyond the Standard Model (BSM) that could account for these observations has become a popular area of research in particle physics.

One particular anomaly, which has been of interest for a long time, is the gyromagnetic ratio of the electromagnetic interaction of leptons, especially for muon (μ). There seems to be a 4.2σ discrepancy between the SM prediction and the latest measurement at the E989 experiment at Fermi National Laboratory (FNAL) [4]. This discrepancy was at 3.7σ in the earlier observation at the Brookhaven National Laboratory (BNL) [10]. The solution to this long-term discrepancy between the SM prediction and the experimentally observed value exist in many new physics (NP) scenarios. The most popular ones invoke new particles and/or symmetries that provide additional contributions to the SM prediction. There are, for example, the popular nonsupersymmetric models with single-field extensions are Z' models [11–18], singlet-scalar extension [19–22], vectorlike lepton (VLLs) [23–31], or extensions of the Higgs doublet to two [32–38] or more doublets. While these extensions might give rise to enough contribution to the anomalous magnetic moment of μ, they also contribute to the lepton flavor violation. Since we do not have any evidence for any lepton flavor violation (LFV), simultaneously achieving both goals in a simplistic and universal model is difficult. The usual way around this is to consider nonuniversal couplings of the new particles with the SM particles. There are models with two-particle extensions where it is relatively easy to explain muon anomaly and nonobservation of LFV at the same time [39–42]. The most popular two-particle extensions usually consider a combination of scalars and fermions. For the lepton sector analysis, the fermion is usually a VLL. In addition to such extensions, other ideas also have possible explanations for the $(g-2)_\mu$ anomaly. These ideas mainly include extra-dimensional models [43,44], technicolor models [45], composite models [46–49], leptoquark models [50,51], etc. In this work, we attempt to explain the $(g-2)_\mu$ anomaly while allowing solutions to some of the

*niveditaghosh@hri.res.in
†skrai@hri.res.in
‡tousik.pdf@iiserkol.ac.in

observed flavor anomalies by extending the SM particle content. In our scenario, we have a scalar leptoquark, a real scalar singlet, and a pair of VLLs added to the SM [52,53]. The leptoquark and singlet scalar usually contribute to the magnetic moment of muon via the chiral breaking terms which are proportional to the mass of the heavy particle running in the loop. The VLL is responsible in giving necessary couplings to the μ, τ, and e, so that we get significant contribution to the $(g-2)_\mu$, while the LFV does not receive any large contributions. In our scenario, due to an explicit $\mathbb{Z}_2$ symmetry the scalar leptoquark is instrumental in only addressing the meson flavor anomalies but the VLL and singlet scalars contribute to muon anomaly as well as LFV at one-loop. This model was considered before for explaining various flavor anomalies, for example, $R_D^{(*)}$, $b \to s\mu\mu$, $B_s - \overline{B_s}$ oscillation [53]. In addition, the presence of a neutral scalar or the lightest neutral component of the VLL also explains the dark matter puzzle where the neutral scalar or fermion play the role of dark matter. The presence of a leptoquark and charged VLL in the model also lead to interesting collider signals. We note that most models (unlike ours), introduce a leptoquark but do not augment it with an odd $\mathbb{Z}_2$ parity. The absence of the $\mathbb{Z}_2$ parity allows the leptoquark to couple to SM particles singly, which leads to its direct decay to SM final states. These give strong bounds on the leptoquark mass that can be produced via strong interactions at hadron colliders and then reconstructed through the SM decay products [54–57]. In our case, the production of the leptoquark followed by its decay to VLL and quarks lead to a different signal when compared to the studies available in the literature. The VLL then decays to charged SM leptons and a neutral singlet scalar. The decays finally lead us to a signal of dimuon plus dijet with missing transverse energy. We study the viability of observing the signal at the current and future runs of the Large Hadron Collider (LHC) in this work.

The paper is organized as follows. In Sec. II, we describe the model. In Sec. III, we discuss the allowed parameter space of our model that explain the muon anomalous magnetic moment and lepton flavor violations. We discuss the constraints from electroweak precision (EW) measurements in Sec. IV. In Sec. V, we examine the constraints coming from quark flavor-violating processes. We finally look for distinctive collider signals at LHC and discuss our results in Sec. VI and conclude in Sec. VII.

II. MODEL

We propose a new physics model that may resolve several flavor anomalies observed in recent experiments. The model extends the SM particle content by adding new particles that include a leptoquark (Φ), a pair of $SU(2)$ doublets (L_{4L}, L_{4R}), and a real scalar singlet field (S). We augment the SM symmetry with an additional discrete $\mathbb{Z}_2$ symmetry under which all the SM states are even while the new states are odd. The charge of the new fields under the $\mathcal{G} = SU(3)_C \times SU(2)_L \times U(1)_Y \times \mathbb{Z}_2$ is tabulated in Table I.

TABLE I. New fields and their charges.

Particles	$SU(3)_C$	$SU(2)_L$	$U(1)_Y$	$\mathbb{Z}_2$
Φ	3	1	2/3	−1
L_{4L}	1	2	−1/2	−1
L_{4R}	1	2	−1/2	−1
S	1	1	0	−1

The gauge invariant Lagrangian for the BSM sector can be written as

$$\begin{aligned}\mathcal{L} \supset & -M_\Phi^2 \Phi^\dagger \Phi - M_S^2 S^2 - \lambda_{H\Phi} H^\dagger H \Phi^\dagger \Phi - \lambda_{S\Phi} \Phi^\dagger \Phi S^2 \\ & - \lambda_{HS} H^\dagger H S^2 - \lambda_\Phi (\Phi^\dagger \Phi) - \lambda_S S^4 \\ & - \{h_i \overline{L}_{4R} Q_{Li} \Phi^\dagger + h'_j \bar{L}_{4R} L_{Lj} S + M_F \bar{L}_{4L} L_{4R} + \text{H.c.}\},\end{aligned} \tag{1}$$

where H is the SM Higgs doublet, Q_{Li} and L_{Lj}, $(i, j = 1, 2, 3)$ are the SM quark and lepton doublets, respectively. The VLL doublet $L_4 = (\nu_4, \ell_4^-)^T$ has ν_4 and ℓ_4^- as the neutral and charged components, respectively. Since all the new particles are odd and SM particles are even under the unbroken $\mathbb{Z}_2$ symmetry, the odd particles do not mix with the even particles. This prevents any modification to the couplings of the particles in the SM sector as the unbroken $\mathbb{Z}_2$ prevents the scalar S from acquiring a vacuum expectation value (VEV). However, the presence of $\lambda_{H\Phi}$ and λ_{HS} terms lead to modified mass for Φ and S which shift from M_Φ and $\sqrt{2}M_S$ after electroweak symmetry breaking. The absence of mixing between the SM Higgs boson and S keeps the couplings of SM particles with the SM Higgs boson unaffected. The new scalars in the model are taken to be heavier than the SM Higgs boson such that we do not have any additional decay modes of the SM Higgs boson with respect to the SM. However, the effect of these new heavy states which are both colored and electrically charged would appear through loops. This would alter the hgg and $h\gamma\gamma$ effective couplings, which appear at the one-loop level. We further discuss this in Sec. VI.

We note that almost all the properties of the SM scalar sector remain unaffected at the tree-level in this model. There would be corrections to SM interactions at the loop-level, giving the necessary contributions to the muon $(g-2)$ that could explain the anomaly. The terms in the Lagrangian with the Yukawa couplings h_i and h'_j are responsible for these contributions, where $i, j = 1, 2, 3$ represent the generation indices. Note that the Yukawa term in Eq. (1) containing h_i is written in terms of the flavor eigenbasis of quarks which finally mix via the Cabibbo-Kobayashi-Maskawa (CKM) mixing. After CKM mixing,

the couplings of SM quarks in the physical (mass) eigenbasis become

$$h_i^{\rm ph} \to \sum_{j=1}^{3} h_j U^d_{ji}, \tag{2}$$

where U^d is the mixing matrix of down-type quarks. The new Yukawa couplings would also give rise to new contributions to several other phenomena. For example, the presence of the h_i term in the Lagrangian leads to additional contributions to the $K^0 - \overline{K^0}$ and $B^0 - \overline{B^0}$ oscillations. These two oscillation measurements agree well with the SM prediction. Therefore any new physics contribution to the $K^0 - \overline{K^0}$ and $B^0 - \overline{B^0}$ oscillations must be small and will help in constraining the parameters of the BSM model. In our model this is achieved by choosing leptoquark coupling to the first generation quark to be negligible, i.e., $h^{\rm ph}_{1,2} \simeq 0$ [53]. At the same time, there is still room for new physics in the $B^0_s - \overline{B^0_s}$ oscillation data which gives a constraint $|h^{\rm ph}_2 h^{\rm ph}_3| \lesssim 0.65$ [53,58,59].

The lepton sector is affected by the term containing h'_j coupling. Instead of leptoquark, we have a real scalar involved in this coupling. The enhancement in the $(g-2)_\mu$ can be achieved by considering VLL and the real scalar in the loop. At the same time, the lepton flavor violating decay like $\mu \to e\gamma$ should not yield a large value. This can be achieved by taking large values for the h'_2 and keeping other h' negligible. Moreover, if the real scalar is the lightest among all the new states, it may play the role of DM in this model. The possibility of explaining the DM in this model will be discussed in the later part of this article. In this work, we mainly focus on the muon anomaly, lepton and quark flavor violation, and the signatures of the leptoquark at the LHC.

III. MUON ANOMALY AND LEPTON FLAVOR VIOLATION

The gyromagnetic ratio of muon (g_μ) is exactly 2 at the tree-level. However quantum corrections are induced through contributions from higher-order loops within the SM and the deviation from its tree-level value is denoted by $a_\mu = \frac{g_\mu - 2}{2}$, known as the anomalous magnetic moment of the muon. In the SM, the current value reads [60–80]

$$a_\mu^{\rm SM} = 116591810(43) \times 10^{-11}. \tag{3}$$

The recent results from the "Muon $g-2$" at Fermilab [3] from their first run data provides the anomalous magnetic moment to be [4]

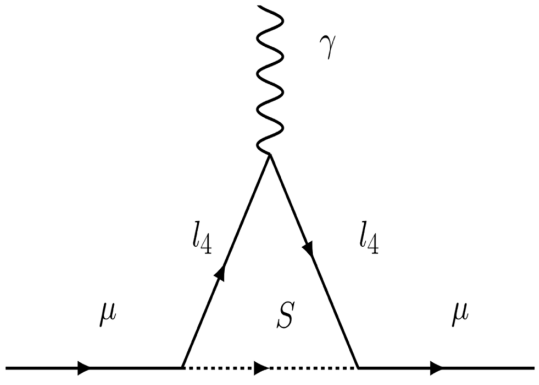

FIG. 1. Feynman diagram for the NP contribution to $(g-2)_\mu$ at one-loop.

$$a_\mu^{\text{exp-FNAL}} = 116592040(54) \times 10^{-11}. \tag{4}$$

The combined new world average (combination of recent FNAL [4] and older BNL(2006) [10] data) is published as [81]

$$a_\mu^{\text{exp-comb}} = 116592061(41) \times 10^{-11}. \tag{5}$$

The difference between the experimental observation and the SM prediction, defined as Δa_μ, amounts to a 4.2σ discrepancy, which provokes one to look beyond the SM.

$$\Delta a_\mu = a_\mu^{\text{exp-comb}} - a_\mu^{\rm SM} = 251(59) \times 10^{-11}. \tag{6}$$

The a_μ is chirality flipping and is generated in our model by the Feynman diagram corresponding to the new physics (NP) contribution at one-loop as shown in Fig. 1. The contribution comes from the scalar S and the VLL in the loop and the expression for Δa_μ is given by [52]

$$\Delta a_\mu = \frac{m_\mu^2 |h'_2|^2}{8\pi^2 M^2_{\ell_4}} f\left(\frac{M_S^2}{M^2_{\ell_4}}\right), \tag{7}$$

where m_μ is the mass of muon and

$$f(x) = \frac{1 - 6x - 6x^2 \ln x + 3x^2 + 2x^3}{12(1-x)^4}. \tag{8}$$

We show the allowed range of the parameter space in Fig. 2 which satisfies the experimental value of Δa_μ within a 3σ range. The parameters in our model are scanned over:

$$M_{\ell_4} \in [102.6 : 500]\ \text{GeV}, \qquad M_S \in [100 : 400]\ \text{GeV}, \qquad h'_2 \in [1 : 3.5] \tag{9}$$

to highlight the regions of parameter space which can explain the $(g-2)_\mu$ observation. The mass of the charged lepton M_{ℓ_4} has a lower bound of 102.6 GeV from Large

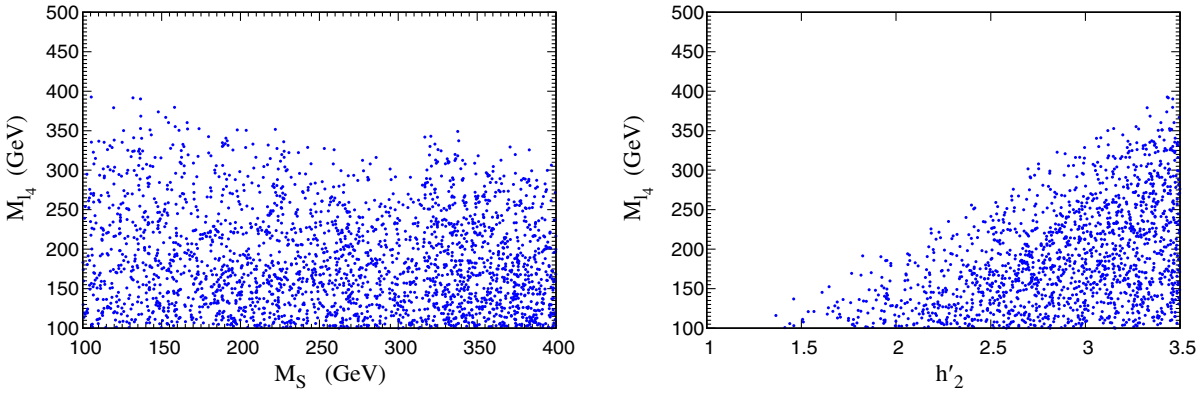

FIG. 2. The allowed parameter space satisfying muon anomaly in (a) $M_S - M_{\ell_4}$ and (b) $h'_2 - M_{\ell_4}$ plane. For these plots, we have varied the parameter as given in Eq. (9).

Electron Positron collider (LEP) [59] and hence, in the scan, the lower range of M_{ℓ_4} has been set to this value. From Fig. 2(a), we see that $M_{\ell_4} \lesssim 400$ GeV is preferred to satisfy the muon anomaly data. Larger values of M_{ℓ_4} would render the Yukawa coupling h'_2 nonperturbative. The allowed values for the scalar mass can be, however, equal, heavier or lighter than the VLL mass. In our model, we preferably set the scalar S to be the DM candidate, which sets $M_S < M_{\ell_4}$. It is worth pointing out that the leptoquark mass M_Φ does not play any role which is expected, as the leptoquark which is odd under $\mathbb{Z}_2$ will not contribute at one-loop. The anomaly prefers a large value for the Yukawa coupling as one can see from Fig. 2(b). We find that $h'_2 \gtrsim 1.5$ are more favorable for all mass values of the VLL. The parameters that explain the muon anomaly are chosen for our collider analysis which we discuss later in Sec. VI.

We note that similar diagrams as the muon anomaly diagram, with external muons replaced by appropriate leptons, will contribute to the LFV decay modes. Though the violation of lepton flavor has been observed in neutrino oscillation [82,83], nonobservation of any significant LFV in the charged lepton sector put strong constraints on LFV processes. The strongest bound in the μ–e sector ($\mathrm{BR}(\mu \to e\gamma) < 4.2 \times 10^{-13}$) comes from the MEG experiment [5]. Similar to the μ–e sector, we also get constraints from $(\tau \to e\gamma)$ and $(\tau \to \mu\gamma)$ decay branching ratios (BR). The current bound on these lepton flavor conversions are [6]

$$\mathrm{BR}(\tau \to e\gamma) < 3.3 \times 10^{-8}, \quad \mathrm{BR}(\tau \to \mu\gamma) < 4.4 \times 10^{-8}.$$

As pointed out before, these constraints can be avoided easily in our model by choosing h'_1 and h'_3 small. We choose values for these parameters in the following range: $h'_1 \in [10^{-5} : 10^{-4}]$, and, $h'_3 \in [0.01 : 0.1]$ which are allowed by the above LFV constraints.

IV. ELECTROWEAK PRECISION MEASUREMENT

We note that the observed anomalous magnetic moment of the muon and $R_K^{(*)}$ anomaly prefers a relatively large value of h'_2 in our model. A large Yukawa coupling could have several unwanted consequences as it can lead to large contributions to various subprocesses within the SM, even when the new physics particles appear in the loops. We already discussed how our model avoids LFV constraints but an immediate concern arises from electroweak precision measurements at the Large Electron-Positron Collider (LEP). The choice of large values for h'_2 cannot only cause corrections for the muon mass but also alter the SM $Z\mu^+\mu^-$ coupling, which was precisely determined at LEP. In our model, the additional contribution to the interaction vertex of $Z\mu^+\mu^-$ comes from a similar one-loop diagram shown in Fig. 1. The relative change of $Z\mu^+\mu^-$ coupling with respect to its SM value can be expressed as

$$\frac{\delta g_L^\mu}{g_{L,\mathrm{SM}}^\mu}(q^2) = \frac{q^2}{32\pi^2 M_{\ell_4}^2} |h'_2|^2 G\left(\frac{M_S^2}{M_{\ell_4}^2}\right), \tag{10}$$

where q is the momenta carried by the Z boson and the loop function

$$G(x) = \frac{7 - 36x + 45x^2 - 16x^3 + (12x^3 - 18x^2)\log x}{36(x-1)^4} \tag{11}$$

From the LEP, the upper limit for the absolute value of $\delta g_L^\mu / g_{L,\mathrm{SM}}^\mu (q^2 = M_Z^2)$ is 0.8% [52]. For our model, we plotted a contour plot of $|\delta g_L^\mu / g_{L,\mathrm{SM}}^\mu (q^2 = M_Z^2)|$ as function of M_S and M_{l_4} in Fig. 3 with $h'_2 = 3.0$. The number on the contour lines represent the value of $|\delta g_L^\mu / g_{L,\mathrm{SM}}^\mu (q^2 = M_Z^2)|$ in our model. As can be seen from Fig. 3, within the range of the contour plot, the relative change of $Z\mu^+\mu^-$ coupling

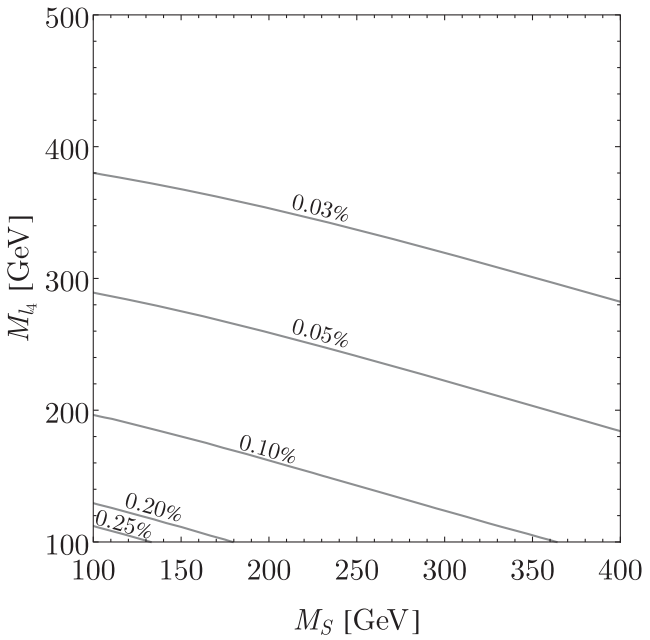

FIG. 3. Contour plot of $|\delta g_L^\mu / g_{L,\mathrm{SM}}^\mu(q^2 = M_Z^2)|$ as a function of M_S and M_{l_4} with $h_2' = 3.0$.

due to new physics is always less than 0.3%. Since we are interested in the mass range $M_S > 100$ GeV and $M_{l_4} > 100$ GeV, we are safe from the LEP constraints in the range of parameters which we shall use for our LHC analysis that can simultaneously explain the muon anomaly.

V. QUARK FLAVOR VIOLATION

The presence of leptoquarks and their interactions with SM quarks and leptons can also induce flavor-violating decays of hadrons. As pointed out earlier, the terms containing h_i and h_i' couplings induce extra contributions to flavor violation in the quark sector via loop. In this work, we consider the one-loop contribution to the quark flavor violation (QFV), primarily focusing on the constraints coming from $b \to s$ transition, observed in the decays of B meson. The quark level transitions in such decays arise primarily from three modes, viz. (i) $b \to s\ell^+\ell^-$, (ii) $b \to s\bar{\nu}\nu$, and (iii) $b \to s\gamma$. In addition to B meson decays, the $B_s - \bar{B}_s$ mixing also provides the information for $b \to s$ transition.

We first provide a brief account of the recent experimental results and SM predictions for $b \to s$ transition. The most recent observation for $b \to s\ell^+\ell^-$ transition comes from the measurement of the ratio

$$R_{K^{(*)}} = \frac{\mathrm{BR}(B \to K^{(*)}\mu^+\mu^-)}{\mathrm{BR}(B \to K^{(*)}e^+e^-)}$$

by LHCb [7]. The measurement is in tension with SM and stands 2.6σ away from the SM prediction [84]. The $b \to s\bar{\nu}\nu$ transition is constrained from $B \to K^{(*)}\bar{\nu}\nu$ transition [85] and our model gives no additional contribution to this mode. The meson decay $B \to X_s\gamma$ provides constraints on $b \to s\gamma$ transition. The current experimental result and SM prediction for this decay probability $\mathrm{BR}(b \to s\gamma)$ are $(3.43 \pm 0.21 \pm 0.07) \times 10^{-4}$ [8] and $(3.36 \pm 0.23) \times 10^{-4}$ [86], respectively. In the $B_s - \bar{B}_s$ system, the experimental result for ΔM_{B_s} is 1σ below the SM prediction [9].

From the theory side, the relevant NP contributions to $b \to s\mu^+\mu^-$ come from the following effective Hamiltonian

$$\mathcal{H} \supset -\frac{\alpha_{\mathrm{em}} G_F}{\sqrt{2}\pi} V_{tb} V_{ts}^* (C_9 \mathcal{O}_9 + C_{10}\mathcal{O}_{10}), \tag{12}$$

where α_{em} and G_F are fine-structure constant and Fermi constant, respectively. V_{tb} and V_{ts} are CKM matrix elements and C_9 and C_{10} are the Wilson coefficients of the operators

$$\mathcal{O}_9 = (\bar{s}\gamma^\alpha P_L b)(\bar{\mu}\gamma_\alpha \mu), \quad \mathcal{O}_{10} = (\bar{s}\gamma^\alpha P_L b)(\bar{\mu}\gamma_\alpha\gamma_5\mu). \tag{13}$$

For $b \to s\gamma$, the NP contribution comes from the effective Hamiltonian

$$\mathcal{H} \supset -\frac{m_b G_F}{4\sqrt{2}\pi^2} V_{tb} V_{ts}^* (C_7 \mathcal{O}_7 + C_8 \mathcal{O}_8), \tag{14}$$

where m_b is the mass of bottom quark and C_7 and C_8 are Wilson coefficients corresponding to the operators

$$\mathcal{O}_7 = e(\bar{s}\sigma^{\mu\nu} P_R b) F_{\mu\nu}, \quad \mathcal{O}_8 = g_s(\bar{s}\sigma^{\mu\nu} T^a P_R b) G^a_{\mu\nu}. \tag{15}$$

For the $B_s - \bar{B}_s$ mixing, the effective Hamiltonian is given by

$$\mathcal{H} \supset C_{B\bar{B}}(\bar{s}\gamma^\mu P_L b)(\bar{s}\gamma_\mu P_L b). \tag{16}$$

The constraints coming from experimental measurements can then be translated to give constraints on the above Wilson coefficients. The combined fit provides the following bounds on the Wilson coefficients [52].

$$\begin{aligned} -1.14 \le C_9 = -C_{10} \le -0.23 \quad & (3\sigma), \\ -2.8 \le C_{B\bar{B}} \times (10^5\ \mathrm{TeV}^2) \le 1.3 \quad & (3\sigma), \\ -0.098 \le C_7 + 0.24 C_8 \le 0.070 \quad & (2\sigma). \end{aligned} \tag{17}$$

For this model, the NP contribution to these Wilson coefficients can be obtained using the expressions given in Ref. [52]. One, of course, needs to ensure that the Wilson coefficients satisfy the bounds given in Eq. (17). This can be ensured by choosing appropriate values for h_2 and h_3 couplings which will be briefly discussed in the next section.

TABLE II. The benchmark points and the production cross sections at 14 TeV LHC are shown in columns (2–5). The corresponding Wilson coefficients [Eq. (17)] are given in columns (6–8). The Higgs boson signal strength is also provided in the last column.

	M_Φ (GeV)	M_{ℓ_4} (GeV)	M_S (GeV)	$\sigma_{LO}(pp \to \Phi\bar{\Phi})$ (fb)	C_9 $(-C_{10})$	$C_{B\bar{B}}$ (TeV^2)	$C_7 + 0.24C_8$	$\mu_{\gamma\gamma}$
BP1	750.8	280.0	244.9	33.61	−1.03	0.07×10^{-5}	−0.006	0.98
BP2	826.8	290.0	260.0	17.44	−0.90	0.05×10^{-5}	−0.005	0.98
BP3	902.02	300.0	270.0	9.8	−0.79	0.04×10^{-5}	−0.004	0.98
BP4	1001.8	320.0	282.8	5.0	−0.67	0.03×10^{-5}	−0.003	0.98

VI. COLLIDER SEARCHES

In this section, we look at the collider signatures in our model. The most interesting signal comes from the leptoquark production. Since the leptoquark is $\mathbb{Z}_2$ odd its signals will not only entail a baryon and lepton number violation but also give large missing transverse momentum due to the presence of a final $\mathbb{Z}_2$ odd state in its decay cascade, which will go undetected. For this study we shall focus on the parameter space which can account for both muon anomaly and satisfy constraints coming from lepton and quark flavor violation.

We consider the pair production process of the leptoquark.

$$pp \to \Phi\bar{\Phi} \tag{18}$$

The leptoquark carries charge $Q_{em} = +2/3$ and therefore can decay to both up-and down-type quark flavor. A few interesting points about the leptoquark in our model is worth highlighting before we discuss the signals arising from its production at LHC. Due to the unbroken $\mathbb{Z}_2$ parity, the leptoquark is forced to decay to a SM quark and the new exotic lepton. This leads to an interesting possibility where its decay may not remain within the same fermion generation. This is because the VLL (L_4) couples more strongly to muon and the scalar S compared to the other SM leptons. This enabled our model to account for the muon anomaly as discussed earlier. Note that the leptoquark, which couples mostly to the third generation of SM quarks, is weakly constrained compared to the leptoquarks which couple to the first two generations. We therefore consider the leptoquarks which have larger coupling to third generation SM quark and the exotic lepton. In such a case, and if kinematically allowed, the decay modes of the leptoquark will be as follows:

$$\Phi \to b\ell_4^+ \to b\mu^+ S \to t\bar{\nu}_4 \to bW^+\nu S$$

As a multilepton final state at LHC will be much more clean, we will consider only the leptonic decay of the W boson.[1] The collider signature of our interest then becomes a final state given by $2\mu + 2b + \not{E}_T$. The SM subprocesses that can give rise to the same final state are dominated by the inclusive $t\bar{t}(+1jet)$ with at least one extra hard jet,[2] and subdominant contributions come from the $t\bar{t}h$, $t\bar{t}V$, VV, and VVV, where $V = W^\pm, Z$. In principle, the diboson plus dijets can also be a source of the background if both the light jets are mistagged as b-jet. However, the mistagging efficiency of a light jet identified as a b-jet is ≈1% for u, d, s and ≈10% for the c quark. In addition the production cross section is much smaller than the inclusive $t\bar{t}(+1jet)$ background. We also note that the requirement of a high p_T b-jet removes almost all of this background. For our analysis, we have chosen four benchmark points. We list them and the corresponding pair-production cross sections for the leptoquark in Table II. For all the benchmark points, we have fixed the h_i and h_i' couplings which are shown in Table III. We have ensured that the benchmark points satisfy the bounds discussed in Secs. III–V. For the QFV bounds, the values of the Wilson coefficients have also been tabulated in Table II. These values are within the bounds provided in Eq. (17).

TABLE III. The values of the Yukawa-type couplings kept fixed for all the benchmark points.

h_1	h_2	h_3	h_1'	h_2'	h_3'
0.01	−0.01	0.52	5.0×10^{-5}	3.0	0.01

For the scalar sector, the modification of Higgs boson couplings is measured experimentally in terms of Higgs boson signal strength, which is defined, in the $\gamma\gamma$ channel, as

$$\mu_{\gamma\gamma} = \frac{[\sigma(pp \to h) \times \mathrm{BR}(h \to \gamma\gamma)]_{\mathrm{exp}}}{[\sigma(pp \to h) \times \mathrm{BR}(h \to \gamma\gamma)]_{\mathrm{SM}}}, \tag{19}$$

where $\sigma(pp \to h)$ is the production cross section of the Higgs and BR denotes the branching ratio of the Higgs boson decaying to two photons. In our model, we have calculated the values of the $\mu_{\gamma\gamma}$ using the effective hgg and $h\gamma\gamma$ couplings [88–90]. For the four benchmark points, we

[1]Hadronic decays of the W boson will provide lower sensitivity due to the presence of huge QCD background.

[2]To generate this particular background, we have generated the $pp \to t\bar{t}$ and $pp \to t\bar{t}j$ in MadGraph [87] and used MLM matching scheme for the additional jet.

provide these values in Table II. These values lie well within the 2σ range of the CMS data 1.1 ± 0.08 [91].

The standard search for scalar leptoquarks at the collider experiments are carried out by looking at the $2\ell + 2j$ channels [54–57]. These searches generally assume that the leptoquarks couple to a SM lepton and a SM quark. For such an assumption the leptoquark can be produced singly and in a pair and the decay of the leptoquark will give no missing transverse momenta when the decay contains a charged SM lepton. As expected, selection cuts on $\not{E}_T$ are usually kept low for such scenarios. On the other hand, in our model, the leptoquark couples to a SM quark and a BSM VLL, owing to the discrete $\mathbb{Z}_2$ parity. This BSM lepton then decays to a scalar DM and a SM lepton. As a result, in our model, one expects large $\not{E}_T$ from the decay of leptoquark. Therefore, the current searches for leptoquark at the LHC do not put very strong constraints on our model parameters. In some cases, the leptoquark has been studied in the $2\ell + 2t$ channel [57,92,93], where one expects a little more $\not{E}_T$, if the top quark decays leptonically. However, these searches also do not constrain the model parameters of our model significantly.

Interestingly, the search for the leptoquark in this particular channel $(2\mu + 2b + \not{E}_T)$ has been carried out by the ATLAS and CMS collaborations at the 13 TeV LHC run [94–97]. The strongest bound comes from the search for top squark pair production in the same channel [94] and hence this analysis when recasted for our model, could constrain our model parameters as well. We have scanned our model parameters using the recasting tool, i.e., the CheckMATE [98] package and have realized that leptoquarks, heavier than 750 GeV are not excluded by the above search at 95% C.L. We have also checked that all the benchmark points are allowed by the above search.

Since we demand that the BSM particles are odd under $\mathbb{Z}_2$ symmetry, the lightest particle may become the DM candidate. In the above four benchmark points, the real scalar S is the lightest $\mathbb{Z}_2$ odd particle and hence it plays the role of DM candidate. To study the DM phenomenology, the CalcHEP [99] compatible model files are obtained from SARAH [100] and then included in micrOMEGAs [101], which calculates the DM observables like relic density $\Omega_{\rm DM}h^2$, spin-dependent ($\sigma_{\rm SD}$) and spin-independent ($\sigma_{\rm SI}$) cross sections, and the thermally averaged annihilation cross sections ($\langle\sigma v\rangle$). As the scalar DM does not couple with the nucleons, the direct detection constraints are easily satisfied in our model. We also find that our benchmark points are compatible with relic abundance obtained from the PLANCK experiment [102]. For our four benchmark points, BP1, BP2, BP3, and BP4, the relic density is $7.79 \times 10^{-3}, 4.16 \times 10^{-3}, 3.98 \times 10^{-3}$, and 7.28×10^{-3} respectively. This suggests that the DM is underabundant for these benchmark points. However, tuning the Yukawa coupling (h') parameters could give us the correct relic abundance. Since we are more interested in the leptoquark signal at LHC, we postpone the discussion about dark matter for separate work.

For the LHC analysis, we implement the model file in SARAH [100] and generate the required UFO which is used to generate events in MadGraph [87]. The spectrum files for the benchmark points are generated using SPheno [103]. The events generated in MadGraph are then passed on to PYTHIA8 [104] for showering and hadronization. The detector simulation is done in DELPHES [105] using the default CMS card, where the jets are constructed using the anti-K_T algorithm with a jet formation radius of $R = 0.4$. For the SM background processes with hard jets, proper MLM matching scheme [106] has been applied. The charged leptons in the final state are isolated by choosing $\Delta R_{\ell i} > 0.4$, where i represents either a jet or a lepton. For generating signal and background events at the parton level, we use the following kinematic acceptance cuts on the partons and leptons (electron and muon):

$$\begin{aligned} &p_T(j,b) > 20\ \text{GeV}; \qquad |\eta(j)| < 4.7; \qquad |\eta(b)| < 2.5, \\ &p_T(\ell) > 10\ \text{GeV}, \qquad |\eta(\ell)| < 2.5. \end{aligned} \tag{20}$$

The b-jets are tagged using a p_T dependent efficiency given as

$$\epsilon_b = 0.85\ \tanh(0.0025\mathrm{p_T})\frac{25.0}{(1+0.063\mathrm{p_T})}.$$

Similarly a mistagging efficiency for c-jets being wrongly identified as b jets, given by

$$\epsilon_{c\to b} = 0.25\ \tanh(0.018\mathrm{p_T})\frac{1}{(1+0.0013\mathrm{p_T})},$$

is included and a mistag efficiency of $\epsilon_{l\to b} = (0.01 + 0.000038\mathrm{p_T})$ for the light jets is also included.

We now provide the details of our cut-based analysis of the signal and SM background events, which maximize the signal to background ratio. Along with the basic cuts mentioned in Eq. (20), we put additional selection cuts on the following kinematic variables as described below:

(i) $\mathbf{p_T}(\mu)$: We depict the p_T distribution of the leading and subleading muon in Figs. 4(a) and 4(b), respectively. As our signal contains two muons, we select one leading and one subleading muon with transverse momentum $p_T > 10$ GeV and reject events containing more than two muons. We can see that the signal and background events peak in the same p_T range. We find that the muon in the signal events have a p_T cut-off dependent on the mass of the VLL. Therefore a lower cut on the p_T does not help to reduce the background. Instead, an upper cut on the leading muon $p_T(\mu_1) < 180$ GeV is helpful in removing the SM tail and improving the signal sensitivity.

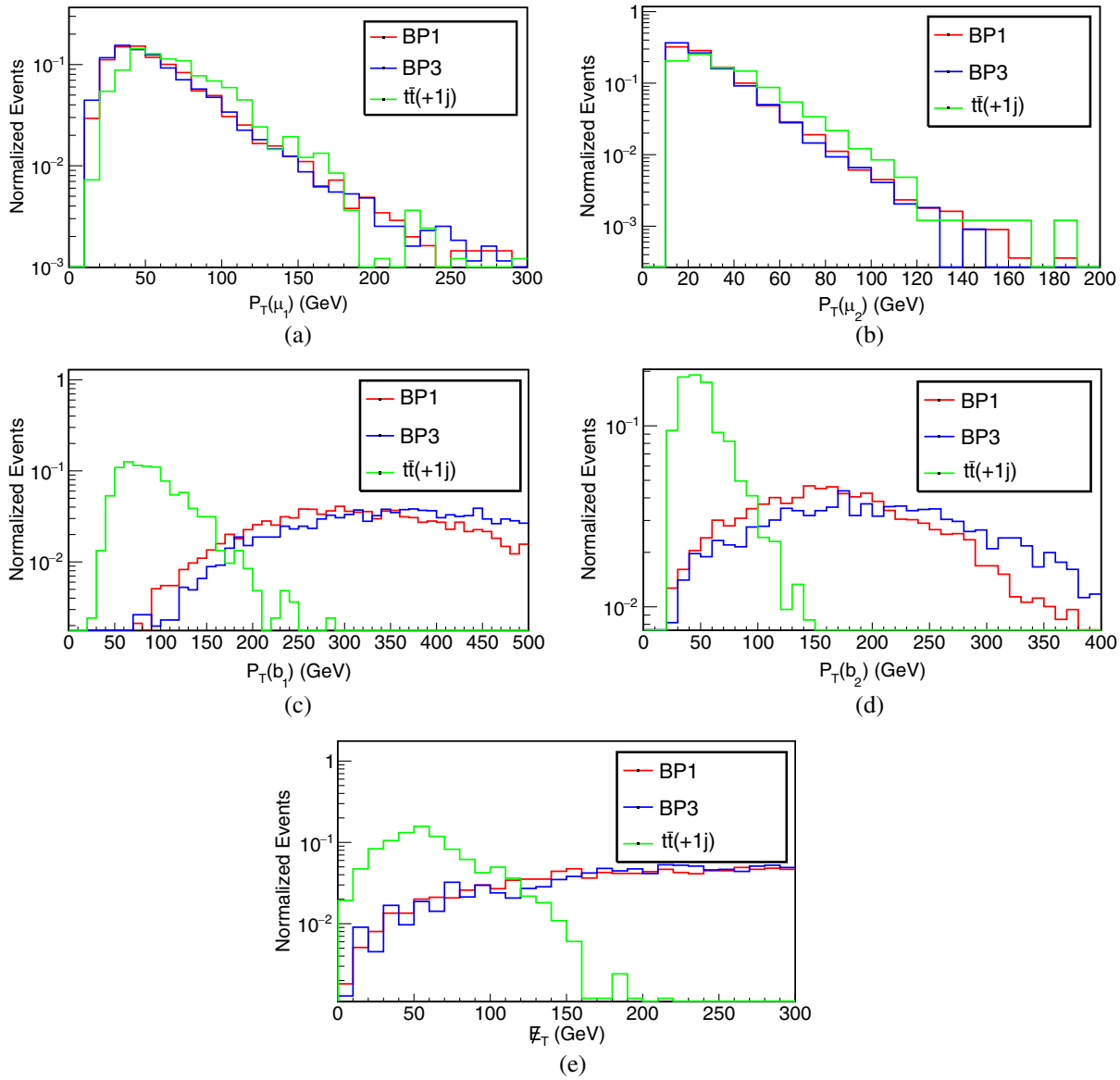

FIG. 4. Normalized distribution of the kinematic variables for the signal and dominant SM background.

(ii) $\mathbf{p_T(b)}$: We show the normalized p_T distribution for the leading and subleading b-jet in Figs. 4(c) and 4(d), respectively. To ensure that our signal contains only two b-jets, we reject events with a third b-jet with $p_T > 20$ GeV. For the background, the b-jets come from the decay of top quark, whereas for the signal the b-jets come directly from much heavier leptoquarks. So the signal distribution peaks at a higher value compared to the SM background. We put a lower cut on the transverse momentum $p_T(b_1) > 200$ GeV and $p_T(b_1) > 100$ GeV to enhance the signal over background. This cut also helps in drastically suppressing the $t\bar{t}V$ and diboson + dijet backgrounds, finally leaving us with background events coming dominantly from the inclusive $t\bar{t}(+1jet)$ production in SM.

(iii) $\not{E}_{\mathbf{T}}$: The $\not{E}_T$ distribution is plotted in Fig. 4(e). As our signal contains a heavy dark matter scalar candidate S, the $\not{E}_T$ peaks at a higher value in contrast to the background where the $\not{E}_T$ comes only from the neutrinos arising from the $W^{\pm}$ decay. We put a lower cut on missing transverse energy as $\not{E}_T > 200$ GeV to suppress the SM background further.

The detailed outcome of our cut-flow choice for different benchmark points is shown in Table IV.

The signal significance is then calculated by using the formula [107]

$$\mathcal{S} = \sqrt{2\left[(S+B)\log\left(\frac{S+B}{B}\right) - S\right]}, \tag{21}$$

TABLE IV. The cut-flow for signal and backgrounds for $2\mu + 2b + \not{E}_T$ channel along with the significance for benchmarks BP1, BP2, BP3, and BP4 to be probed at 14 TeV LHC with 3000 fb^{-1} luminosity.

	Number of Events after cuts ($\mathcal{L} = 3000$ fb^{-1})			
SM-background	$p_T(\mu_1)$ cut	$p_T(b)$ cut	$\not{E}_T$ cut	
$t\bar{t}(+1jet)$	974682	8361	717	
$t\bar{t}V$	585	32	5	
$VVjj + VVb\bar{b}$	9223	41	15	
Total background	984490	8434	737	
Signal				Significance reach at 3000 fb^{-1}
BP1	546	318	318	11.0σ
BP2	244	199	160	5.7σ
BP3	125	105	88	3.2σ
BP4	57	51	45	1.6σ

where $S(B)$ represents the number of signal (background) events surviving after all the cuts are applied. It can be seen from Table IV that, as the leptoquark mass increases, the signal significance decreases Although the cut efficiencies are more useful for the signal coming from the heavier states, the production cross section falls as shown in Table II. We find that it will be possible to probe the benchmark points BP1, BP2, and BP3 with statistical significance of $11.0\sigma, 5.7\sigma, 3.2\sigma$ respectively, while BP4 with the leptoquark mass of 1 TeV gives a 1.6σ statistical significance with 3000 fb^{-1} integrated luminosity.

VII. CONCLUSION

The observation of muon and flavor anomalies has generated a lot of renewed interest in new ideas of BSM physics in the particle physics community. The extension of SM by new fields usually provides contributions to these anomalies via higher-order loops.

In this work, we have studied a model which extends the SM by a scalar leptoquark, one generation of VLL and one SM singlet scalar. The new fields are odd under a $\mathbb{Z}_2$ symmetry. By virtue of this $\mathbb{Z}_2$ symmetry the scalar or the lightest neutral VLL acts as a DM candidate. Any mixing with the SM fields is also avoided due to this discrete parity being unbroken in the model. The new fields couple to the SM particles via Yukawa-type interactions. The VLL and the scalar contribute to the anomalous magnetic moment of muon at the one-loop. We see that for a significant range of the parameter space, this anomaly can be satisfied within the 3σ error bar of the current data. The Yukawa interaction also provides an extra contribution to the LFV. We check for parameter space that is allowed by all such LFV constraints and QFV constraints, namely $b \to s\mu\mu$, $b \to s\gamma$, and $B_s - \overline{B_s}$ mixing.

We then chose representative benchmark points for leptoquark mass and look for a distinct signal in $2\mu + 2b + \not{E}_T$ final states which can be probed at the 14 TeV LHC run. We also note that the chosen benchmark points satisfy DM constraints as well as account for the measured muon anomaly. Based on a simple cut-based analysis we find that most of the benchmark points lead to signals with more than 3σ significance at 3000 fb^{-1} integrated luminosity. We also conclude that a scalar leptoquark with masses above $\gtrsim 1$ TeV would be difficult to observe in the simple-minded cut-based analysis and may require more sophisticated machine-learning methods to have any chance of observation. Our analysis also shows that current limits on the scalar leptoquarks which decay directly to SM particles would become much weaker in the presence of nonstandard decays of the leptoquark. This can be a highly probable scenario if one considers explaining the flavor and muon anomalies in a common setup and looks at the collider signatures of such a model.

ACKNOWLEDGMENTS

N. G. and S. K. R. would like to thank the Regional Centre for Accelerator-based Particle Physics (RECAPP), Harish-Chandra Research Institute, Department of Atomic Energy, Government of India for financial support. T. S. would like to acknowledge RECAPP for providing hospitality when this work was ongoing.

[1] G. Aad *et al.* (ATLAS Collaboration), Observation of a new particle in the search for the Standard Model Higgs boson with the ATLAS detector at the LHC, Phys. Lett. B **716**, 1 (2012).

[2] S. Chatrchyan *et al.* (CMS Collaboration), Observation of a new boson at a mass of 125 GeV with the CMS experiment at the LHC, Phys. Lett. B **716**, 30 (2012).

[3] J. Grange *et al.* (Muon $g-2$ Collaboration), Muon (g-2) technical design report, arXiv:1501.06858.

[4] T. Albahri *et al.* (Muon $g-2$ Collaboration), Measurement of the anomalous precession frequency of the muon in the Fermilab Muon $g-2$ experiment, Phys. Rev. D **103**, 072002 (2021).

[5] A. M. Baldini *et al.* (MEG Collaboration), Search for the lepton flavour violating decay $\mu^+ \to e^+\gamma$ with the full

dataset of the MEG experiment, Eur. Phys. J. C **76**, 434 (2016).
[6] B. Aubert *et al.* (*BABAR* Collaboration), Searches for Lepton Flavor Violation in the Decays $\tau^{\pm} \to e^{\pm} \gamma$ and $\tau^{\pm} \to \mu^{\pm} \gamma$, Phys. Rev. Lett. **104**, 021802 (2010).
[7] R. Aaij *et al.* (LHCb Collaboration), Test of Lepton Universality Using $B^{+} \to K^{+}\ell^{+}\ell^{-}$ Decays, Phys. Rev. Lett. **113**, 151601 (2014).
[8] Y. Amhis *et al.* (Heavy Flavor Averaging Group (HFAG) Collaboration), Averages of b-hadron, c-hadron, and τ-lepton properties as of summer 2014, arXiv:1412.7515.
[9] A. Bazavov *et al.* (Fermilab Lattice and MILC Collaboration), $B^0_{(s)}$-mixing matrix elements from lattice QCD for the Standard Model and beyond, Phys. Rev. D **93**, 113016 (2016).
[10] G. W. Bennett *et al.* (Muon $g-2$ Collaboration), Final report of the E821 muon anomalous magnetic moment measurement at BNL, Phys. Rev. D **73**, 072003 (2006).
[11] W.-C. Chiu, C.-Q. Geng, and D. Huang, Correlation between muon $g-2$ and $\mu \to e\gamma$, Phys. Rev. D **91**, 013006 (2015).
[12] M. Bauer and M. Neubert, Minimal Leptoquark Explanation for the $R_{D^{(*)}}$, R_K, and $(g-2)_\mu$ Anomalies, Phys. Rev. Lett. **116**, 141802 (2016).
[13] E. Coluccio Leskow, G. D'Ambrosio, A. Crivellin, and D. Müller, $(g-2)\mu$, lepton flavor violation, and Z decays with leptoquarks: Correlations and future prospects, Phys. Rev. D **95**, 055018 (2017).
[14] A. Datta, J. L. Feng, S. Kamali, and J. Kumar, Resolving the $(g-2)_\mu$ and B anomalies with leptoquarks and a dark Higgs boson, Phys. Rev. D **101**, 035010 (2020).
[15] D. Marzocca and S. Trifinopoulos, Minimal Explanation of Flavor Anomalies: B-Meson Decays, Muon Magnetic Moment, and the Cabibbo Angle, Phys. Rev. Lett. **127**, 061803 (2021).
[16] D. Zhang, Radiative neutrino masses, lepton flavor mixing and muon $g-2$ in a leptoquark model, J. High Energy Phys. 07 (2021) 069.
[17] P. Ko, T. Nomura, and H. Okada, Muon g$-$2, B$\to$K$^{(*)}\mu^{+}\mu^{-}$ anomalies, and leptophilic dark matter in $U(1)_{\mu-\tau}$ gauge symmetry, J. High Energy Phys. 05 (2022) 098.
[18] Y. Cheng, X.-G. He, and J. Sun, Widening the $U(1)_{L_\mu - L_\tau} Z'$ mass range for resolving the muon g $-$2 anomaly, Phys. Lett. B **827**, 136989 (2022).
[19] S. N. Gninenko and N. V. Krasnikov, The SM extensions with additional light scalar singlet, nonrenormalizable Yukawa interactions and $(g-2)_\mu$, EPJ Web Conf. **125**, 02001 (2016).
[20] J. Liu, N. McGinnis, C. E. M. Wagner, and X.-P. Wang, A light scalar explanation of $(g-2)_\mu$ and the KOTO anomaly, J. High Energy Phys. 04 (2020) 197.
[21] B. D. Sáez and K. Ghorbani, Singlet scalars as dark matter and the muon (g $-$2) anomaly, Phys. Lett. B **823**, 136750 (2021).
[22] R. Capdevilla, D. Curtin, Y. Kahn, and G. Krnjaic, Systematically testing singlet models for $(g-2)_\mu$, J. High Energy Phys. 04 (2022) 129.
[23] R. Dermisek and A. Raval, Explanation of the muon $g-2$ anomaly with vectorlike leptons and its implications for Higgs decays, Phys. Rev. D **88**, 013017 (2013).
[24] Z. Poh and S. Raby, Vectorlike leptons: Muon $g-2$ anomaly, lepton flavor violation, Higgs boson decays, and lepton nonuniversality, Phys. Rev. D **96**, 015032 (2017).
[25] A. Crivellin, M. Hoferichter, and P. Schmidt-Wellenburg, Combined explanations of $(g-2)_{\mu,e}$ and implications for a large muon EDM, Phys. Rev. D **98**, 113002 (2018).
[26] A. S. De Jesus, S. Kovalenko, F. S. Queiroz, C. Siqueira, and K. Sinha, Vectorlike leptons and inert scalar triplet: Lepton flavor violation, $g-2$, and collider searches, Phys. Rev. D **102**, 035004 (2020).
[27] W. Abdallah, R. Gandhi, and S. Roy, Understanding the MiniBooNE and the muon and electron $g-2$ anomalies with a light Z' and a second Higgs doublet, J. High Energy Phys. 12 (2020) 188.
[28] M. Frank and I. Saha, Muon anomalous magnetic moment in two-Higgs-doublet models with vectorlike leptons, Phys. Rev. D **102**, 115034 (2020).
[29] E. J. Chun and T. Mondal, Explaining $g-2$ anomalies in two Higgs doublet model with vector-like leptons, J. High Energy Phys. 11 (2020) 077.
[30] N. Chakrabarty, Doubly charged scalars and vector-like leptons confronting the muon g-2 anomaly and Higgs vacuum stability, Eur. Phys. J. Plus **136**, 1183 (2021).
[31] A. Crivellin and M. Hoferichter, Consequences of chirally enhanced explanations of $(\mathrm{g}-2)_\mu$ for $\mathrm{h} \to \mu\mu$ and $\mathrm{Z} \to \mu\mu$, J. High Energy Phys. 07 (2021) 135.
[32] N. Ghosh and J. Lahiri, Revisiting a generalized two-Higgs-doublet model in light of the muon anomaly and lepton flavor violating decays at the HL-LHC, Phys. Rev. D **103**, 055009 (2021).
[33] W. Abdallah, R. Gandhi, and S. Roy, Two-Higgs doublet solution to the LSND, MiniBooNE and muon $g-2$ anomalies, Phys. Rev. D **104**, 055028 (2021).
[34] N. Ghosh and J. Lahiri, Generalized 2HDM with wrong-sign lepton-Yukawa coupling, in light of $g_\mu - 2$ and lepton flavor violation at the future LHC, Eur. Phys. J. C **81**, 1074 (2021).
[35] A. E. C. Hernández, S. F. King, and H. Lee, Fermion mass hierarchies from vectorlike families with an extended 2HDM and a possible explanation for the electron and muon anomalous magnetic moments, Phys. Rev. D **103**, 115024 (2021).
[36] R. Dermisek, K. Hermanek, and N. McGinnis, Muon $g-2$ in two-Higgs-doublet models with vectorlike leptons, Phys. Rev. D **104**, 055033 (2021).
[37] A. E. C. Hernández, S. Kovalenko, M. Maniatis, and I. Schmidt, Fermion mass hierarchy and g $-$ 2 anomalies in an extended 3HDM model, J. High Energy Phys. 10 (2021) 036.
[38] G. Arcadi, A. S. de Jesus, T. B. de Melo, F. S. Queiroz, and Y. S. Villamizar, A 2HDM for the g-2 and dark matter, Nucl. Phys. **B982**, 115882 (2022).
[39] A. Freitas, J. Lykken, S. Kell, and S. Westhoff, Testing the muon g-2 anomaly at the LHC, J. High Energy Phys. 05 (2014) 145.

[40] K. Kowalska and E. M. Sessolo, Expectations for the muon $g-2$ in simplified models with dark matter, J. High Energy Phys. 09 (2017) 112.

[41] L. Calibbi, R. Ziegler, and J. Zupan, Minimal models for dark matter and the muon g − 2 anomaly, J. High Energy Phys. 07 (2018) 046.

[42] P. Athron, C. Balázs, D. H. J. Jacob, W. Kotlarski, D. Stöckinger, and H. Stöckinger-Kim, New physics explanations of a_μ in light of the FNAL muon g − 2 measurement, J. High Energy Phys. 09 (2021) 080.

[43] P. K. Das, Muon anomalous magnetic moment and a lower bound on Higgs mass due to stabilized radion in the Randall-Sundrum model, Int. J. Mod. Phys. A **21**, 5205 (2006).

[44] P. Moch and J. Rohrwild, $(g-2)_\mu$ in the custodially protected RS model, J. Phys. G **41**, 105005 (2014).

[45] A. Doff and C. Siqueira, Composite Higgs models, technicolor and the muon anomalous magnetic moment, Phys. Lett. B **754**, 294 (2016).

[46] P. Das, S. Kumar Rai, and S. Raychaudhuri, Anomalous magnetic moment of the muon in a composite model, arXiv:hep-ph/0102242.

[47] D. K. Hong and D. H. Kim, Composite (pseudo) scalar contributions to muon g − 2, Phys. Lett. B **758**, 370 (2016).

[48] J. M. Cline, B decay anomalies and dark matter from vectorlike confinement, Phys. Rev. D **97**, 015013 (2018).

[49] S. Xu and S. Zheng, Resolving muon g-2 anomaly with partial compositeness, Eur. Phys. J. C **82**, 969 (2022).

[50] A. Crivellin, D. Müller, and F. Saturnino, Flavor phenomenology of the leptoquark singlet-triplet model, J. High Energy Phys. 06 (2020) 020.

[51] A. Bhaskar, A. A. Madathil, T. Mandal, and S. Mitra, Combined explanation of W-mass, muon $g-2$, $R_{K^{(*)}}$ and $R_{D^{(*)}}$ anomalies in a singlet-triplet scalar leptoquark model, Phys. Rev. D **106**, 11 (2022).

[52] P. Arnan, L. Hofer, F. Mescia, and A. Crivellin, Loop effects of heavy new scalars and fermions in $b \to s\mu^+\mu^-$, J. High Energy Phys. 04 (**2017**) 043.

[53] L. Dhargyal and S. K. Rai, Implications of a vector-like lepton doublet and scalar Leptoquark on $R(D^{(*)})$, arXiv: 1806.01178.

[54] G. Aad *et al.* (ATLAS Collaboration), Search for pairs of scalar leptoquarks decaying into quarks and electrons or muons in $\sqrt{s} = 13$ TeV pp collisions with the ATLAS detector, J. High Energy Phys. 10 (2020) 112.

[55] V. M. Abazov *et al.* (D0 Collaboration), Search for scalar leptoquarks in the acoplanar jet topology in $p\overline{p}$ collisions at $\sqrt{s} = 1.96 - \text{TeV}$, Phys. Lett. B **640**, 230 (2006).

[56] M. Aaboud *et al.* (ATLAS Collaboration), Search for scalar leptoquarks in pp collisions at $\sqrt{s} = 13$ TeV with the ATLAS experiment, New J. Phys. **18**, 093016 (2016).

[57] Y. Okumura (ATLAS Collaboration), Search for leptoquarks using the ATLAS detector, Proc. Sci. ICHEP2020 (**2021**) 268.

[58] L. Di Luzio, M. Kirk, and A. Lenz, Updated B_s-mixing constraints on new physics models for $b \to s\ell^+\ell^-$ anomalies, Phys. Rev. D **97**, 095035 (2018).

[59] P. A. Zyla *et al.* (Particle Data Group), Review of particle physics, Prog. Theor. Exp. Phys. **2020**, 083C01 (2020).

[60] T. Aoyama *et al.*, The anomalous magnetic moment of the muon in the standard model, Phys. Rep. **887**, 1 (2020).

[61] T. Aoyama, M. Hayakawa, T. Kinoshita, and M. Nio, Complete Tenth-Order QED Contribution to the Muon $g-2$, Phys. Rev. Lett. **109**, 111808 (2012).

[62] T. Aoyama, T. Kinoshita, and M. Nio, Theory of the anomalous magnetic moment of the electron, Atoms **7**, 28 (2019).

[63] A. Czarnecki, W. J. Marciano, and A. Vainshtein, Refinements in electroweak contributions to the muon anomalous magnetic moment, Phys. Rev. D **67**, 073006 (2003).

[64] C. Gnendiger, D. Stöckinger, and H. Stöckinger-Kim, The electroweak contributions to $(g-2)_\mu$ after the Higgs boson mass measurement, Phys. Rev. D **88**, 053005 (2013).

[65] M. Davier, A. Hoecker, B. Malaescu, and Z. Zhang, Reevaluation of the hadronic vacuum polarisation contributions to the Standard Model predictions of the muon $g-2$ and $\alpha(m_Z^2)$ using newest hadronic cross-section data, Eur. Phys. J. C **77**, 827 (2017).

[66] A. Keshavarzi, D. Nomura, and T. Teubner, Muon $g-2$ and $\alpha(M_Z^2)$: A new data-based analysis, Phys. Rev. D **97**, 114025 (2018).

[67] G. Colangelo, M. Hoferichter, and P. Stoffer, Two-pion contribution to hadronic vacuum polarization, J. High Energy Phys. 02 (2019) 006.

[68] M. Hoferichter, B.-L. Hoid, and B. Kubis, Three-pion contribution to hadronic vacuum polarization, J. High Energy Phys. 08 (2019) 137.

[69] M. Davier, A. Hoecker, B. Malaescu, and Z. Zhang, A new evaluation of the hadronic vacuum polarisation contributions to the muon anomalous magnetic moment and to $\boldsymbol{\alpha(m_Z^2)}$, Eur. Phys. J. C **80**, 241 (2020).

[70] A. Keshavarzi, D. Nomura, and T. Teubner, The $g-2$ of charged leptons, $\alpha(M_Z^2)$ and the hyperfine splitting of muonium, Phys. Rev. D **101**, 014029 (2020).

[71] A. Kurz, T. Liu, P. Marquard, and M. Steinhauser, Hadronic contribution to the muon anomalous magnetic moment to next-to-next-to-leading order, Phys. Lett. B **734**, 144 (2014).

[72] K. Melnikov and A. Vainshtein, Hadronic light-by-light scattering contribution to the muon anomalous magnetic moment revisited, Phys. Rev. D **70**, 113006 (2004).

[73] P. Masjuan and P. Sánchez-Puertas, Pseudoscalar-pole contribution to the $(g_\mu - 2)$: A rational approach, Phys. Rev. D **95**, 054026 (2017).

[74] G. Colangelo, M. Hoferichter, M. Procura, and P. Stoffer, Dispersion relation for hadronic light-by-light scattering: Two-pion contributions, J. High Energy Phys. 04 (2017) 161.

[75] M. Hoferichter, B.-L. Hoid, B. Kubis, S. Leupold, and S. P. Schneider, Dispersion relation for hadronic light-by-light scattering: Pion pole, J. High Energy Phys. 10 (2018) 141.

[76] A. Gérardin, H. B. Meyer, and A. Nyffeler, Lattice calculation of the pion transition form factor with $N_f = 2 + 1$ Wilson quarks, Phys. Rev. D **100**, 034520 (2019).

[77] J. Bijnens, N. Hermansson-Truedsson, and A. Rodríguez-Sánchez, Short-distance constraints for the HLbL contribution to the muon anomalous magnetic moment, Phys. Lett. B **798**, 134994 (2019).

[78] G. Colangelo, F. Hagelstein, M. Hoferichter, L. Laub, and P. Stoffer, Longitudinal short-distance constraints for the

hadronic light-by-light contribution to $(g-2)_\mu$ with large-N_c Regge models, J. High Energy Phys. 03 (2020) 101.
[79] T. Blum, N. Christ, M. Hayakawa, T. Izubuchi, L. Jin, C. Jung, and C. Lehner, The Hadronic Light-by-Light Scattering Contribution to the Muon Anomalous Magnetic Moment from Lattice QCD, Phys. Rev. Lett. **124**, 132002 (2020).
[80] G. Colangelo, M. Hoferichter, A. Nyffeler, M. Passera, and P. Stoffer, Remarks on higher-order hadronic corrections to the muon $g-2$, Phys. Lett. B **735**, 90 (2014).
[81] B. Abi *et al.* (Muon $g-2$ Collaboration), Measurement of the Positive Muon Anomalous Magnetic Moment to 0.46 ppm, Phys. Rev. Lett. **126**, 141801 (2021).
[82] Y. Fukuda *et al.* (Super-Kamiokande Collaboration), Evidence for Oscillation of Atmospheric Neutrinos, Phys. Rev. Lett. **81**, 1562 (1998).
[83] Q. R. Ahmad *et al.* (SNO Collaboration), Direct Evidence for Neutrino Flavor Transformation from Neutral Current Interactions in the Sudbury Neutrino Observatory, Phys. Rev. Lett. **89**, 011301 (2002).
[84] M. Bordone, G. Isidori, and A. Pattori, On the standard model predictions for R_K and R_{K^*}, Eur. Phys. J. C **76**, 440 (2016).
[85] A. J. Buras, J. Girrbach-Noe, C. Niehoff, and D. M. Straub, $B \to K^{(*)}\nu\bar{\nu}$ decays in the standard model and beyond, J. High Energy Phys. 02 (**2015**) 184.
[86] M. Misiak *et al.*, Updated NNLO QCD Predictions for the Weak Radiative B-Meson Decays, Phys. Rev. Lett. **114**, 221801 (2015).
[87] J. Alwall, R. Frederix, S. Frixione, V. Hirschi, F. Maltoni, O. Mattelaer, H.-S. Shao, T. Stelzer, P. Torrielli, and M. Zaro, The automated computation of tree-level and next-to-leading order differential cross sections, and their matching to parton shower simulations, J. High Energy Phys. 07 (2014) 079.
[88] S. Heinemeyer *et al.* (LHC Higgs Cross Section Working Group), Handbook of LHC Higgs cross sections: 3. Higgs properties, arXiv:1307.1347.
[89] D. de Florian *et al.* (LHC Higgs Cross Section Working Group), Handbook of LHC Higgs cross sections: 4. Deciphering the nature of the Higgs sector, arXiv:1610.07922.
[90] ATLAS Collaboration, Combined measurements of Higgs boson production and decay using up to 139 fb^{-1} of proton-proton collision data at $\sqrt{s} = 13$ TeV collected with the ATLAS experiment, Report No. ATLAS-CONF-2021-053, http://cds.cern.ch/record/2789544.
[91] CMS Collaboration, A portrait of the Higgs boson by the CMS experiment ten years after the discovery, Nature (London) **607**, 60 (2022).
[92] G. Aad *et al.* (ATLAS Collaboration), Search for pair production of third-generation scalar leptoquarks decaying into a top quark and a τ-lepton in pp collisions at $\sqrt{s} =$ 13 TeV with the ATLAS detector, J. High Energy Phys. 06 (2021) 179.
[93] A. M. Sirunyan *et al.* (CMS Collaboration), Constraints on models of scalar and vector leptoquarks decaying to a quark and a neutrino at $\sqrt{s} = 13$ TeV, Phys. Rev. D **98**, 032005 (2018).
[94] ATLAS Collaboration, Search for direct top squark pair production and dark matter production in final states with two leptons in $\sqrt{s} = 13$ TeV pp collisions using 13.3 fb^{-1} of ATLAS data, Report No. ATLAS-CONF-2016-076, 2016, http://cds.cern.ch/record/2206249.
[95] ATLAS Collaboration, Search for squarks and gluinos in events with an isolated lepton, jets and missing transverse momentum at $\sqrt{s} = 13$ TeV with the ATLAS detector, Report No. ATLAS-CONF-2016-054, 2016, http://cds.cern.ch/record/2206136.
[96] M. Aaboud *et al.* (ATLAS Collaboration), Search for a scalar partner of the top quark in the jets plus missing transverse momentum final state at $\sqrt{s} = 13$ TeV with the ATLAS detector, J. High Energy Phys. 12 (2017) 085.
[97] CMS Collaboration, Search for new physics in events with two low momentum opposite-sign leptons and missing transverse energy at $\sqrt{s} = 13$ TeV, Report No. CMS-PAS-SUS-16-048, 2017, http://cds.cern.ch/record/2256640.
[98] M. Drees, H. Dreiner, D. Schmeier, J. Tattersall, and J. S. Kim, CheckMATE: Confronting your favourite new physics model with LHC data, Comput. Phys. Commun. **187**, 227 (2015).
[99] A. Belyaev, N. D. Christensen, and A. Pukhov, CalcHEP 3.4 for collider physics within and beyond the standard model, Comput. Phys. Commun. **184**, 1729 (2013).
[100] F. Staub, SARAH, arXiv:0806.0538.
[101] G. Bélanger, F. Boudjema, A. Pukhov, and A. Semenov, micrOMEGAs4.1: Two dark matter candidates, Comput. Phys. Commun. **192**, 322 (2015).
[102] N. Aghanim *et al.* (Planck Collaboration), Planck 2018 results. VI. Cosmological parameters, Astron. Astrophys. **641**, A6 (2020).
[103] W. Porod and F. Staub, SPheno 3.1: Extensions including flavour, CP-phases and models beyond the MSSM, Comput. Phys. Commun. **183**, 2458 (2012).
[104] T. Sjöstrand, S. Ask, J. R. Christiansen, R. Corke, N. Desai, P. Ilten, S. Mrenna, S. Prestel, C. O. Rasmussen, and P. Z. Skands, An introduction to PYTHIA 8.2, Comput. Phys. Commun. **191**, 159 (2015).
[105] J. de Favereau, C. Delaere, P. Demin, A. Giammanco, V. Lemaître, A. Mertens, and M. Selvaggi (DELPHES 3 Collaboration), DELPHES 3, A modular framework for fast simulation of a generic collider experiment, J. High Energy Phys. 02 (2014) 057.
[106] S. Hoeche, F. Krauss, N. Lavesson, L. Lonnblad, M. Mangano, A. Schalicke *et al.*, Matching parton showers and matrix elements, arXiv:ph/0602031.
[107] G. Cowan, K. Cranmer, E. Gross, and O. Vitells, Asymptotic formulae for likelihood-based tests of new physics, Eur. Phys. J. C **71**, 1554 (2011).